

Resonances from perturbations of quantum graphs with rationally related edges

This article has been downloaded from IOPscience. Please scroll down to see the full text article.

2010 J. Phys. A: Math. Theor. 43 105301

(<http://iopscience.iop.org/1751-8121/43/10/105301>)

View [the table of contents for this issue](#), or go to the [journal homepage](#) for more

Download details:

IP Address: 171.66.16.157

The article was downloaded on 03/06/2010 at 08:40

Please note that [terms and conditions apply](#).

Resonances from perturbations of quantum graphs with rationally related edges

Pavel Exner^{1,2} and Jiří Lipovský^{2,3}

¹ Doppler Institute for Mathematical Physics and Applied Mathematics, Czech Technical University, Břehová 7, 11519 Prague, Czech Republic

² Nuclear Physics Institute ASCR, 25068 Řež near Prague, Czech Republic

³ Institute of Theoretical Physics, Faculty of Mathematics and Physics, Charles University, V Holešovičkách 2, 18000 Prague, Czech Republic

E-mail: exner@ujf.cas.cz and lipovsky@ujf.cas.cz

Received 21 December 2009, in final form 21 January 2010

Published 17 February 2010

Online at stacks.iop.org/JPhysA/43/105301

Abstract

We discuss quantum graphs consisting of a compact part and semi-infinite leads. Such a system may have embedded eigenvalues if some edge lengths in the compact part are rationally related. If such a relation is perturbed, these eigenvalues may turn into resonances; we analyze this effect both generally and in simple examples.

PACS numbers: 03.65.-w, 03.65.Aa

(Some figures in this article are in colour only in the electronic version)

1. Introduction

Quantum graphs have attracted much attention recently. The reason is not only that they represent a suitable model for various microstructures, being thus of a direct practical value, but also that they are an excellent laboratory to study a variety of quantum effects. This comes from a combination of two features. On one hand, these models are mathematically accessible since the objects involved are ordinary differential operators. On the other hand, graphs may exhibit a rich geometrical and topological structure which influences behavior of a quantum particle for which such a graph is a configuration space. Nowadays, there is a huge body of literature on quantum graphs and, instead of presenting a long list of references, we restrict ourselves to mentioning the review papers [Ku04,05, Ku08] as a guide to further reading.

One important property of quantum graphs is that—in contrast to usual Schrödinger operators—the unique continuation principle is in general not valid for them: they can exhibit eigenvalues with compactly supported eigenfunctions even if the graph extends to infinity. This property is closely connected with the fact that eigenvalues embedded in the continuous spectrum are on quantum graphs by far less exceptional than for usual Schrödinger operators.

A typical situation when this happens is when the graph contains a loop consisting of edges with rationally related lengths and the eigenfunction has zeros at the corresponding vertices, which prevents it from ‘communicating’ with the rest of the graph.

On the other hand, since such an effect leans on rational relations between the edge lengths, it is unstable with respect to perturbations which change these ratios. The resolvent poles associated with the embedded eigenvalues do not disappear under such a geometric perturbation, though, and one can naturally expect that they move into the second sheet of the complex energy surface producing resonances. The aim of the present paper is to discuss this effect in a reasonably general setting.

We consider a graph consisting of a compact ‘inner’ part to which a finite number of semi-infinite leads are attached. We assume a completely general coupling of wavefunctions at the graph vertices consistent with the self-adjointness requirement. As a preliminary, we will show, generalizing the result of [EL06], that we can speak about resonances without further adjectives because the resolvent and scattering resonances coincide in the present case. We also show how the problem can be rephrased on the compact graph part only by introducing an effective, energy-dependent coupling.

After that we formulate general conditions under which such a quantum graph possesses embedded eigenvalues in terms of the graph geometry (edge lengths) and the matrix of coupling parameters. The discussion of the behavior of embedded eigenvalues is opened by a detailed analysis of two simple examples: those of a ‘loop’ and a ‘cross’ resonator graph. Here we can not only analyze the effect of small-length perturbations but also, using numerical solutions, find the global pole behavior and illustrate several different types of it. Returning to the general analysis in the closing section, we will derive conditions under which the eigenvalues remain embedded, and show that ‘nothing is lost at the perturbation’ in the sense that the number of poles, multiplicity taken into account, is preserved.

2. Preliminaries

2.1. A universal setting for graphs with leads

Let us consider a graph Γ consisting of a set of vertices $\mathcal{V} = \{\mathcal{X}_j : j \in I\}$, a set of finite edges $\mathcal{L} = \{\mathcal{L}_{jn} : (\mathcal{X}_j, \mathcal{X}_n) \in I_{\mathcal{L}} \subset I \times I\}$ and a set of infinite edges $\mathcal{L}_{\infty} = \{\mathcal{L}_{j\infty} : \mathcal{X}_j \in I_{\mathcal{L}}\}$ attached to them. We regard it as a configuration space of a quantum system with the Hilbert space

$$\mathcal{H} = \bigoplus_{L_j \in \mathcal{L}} L^2([0, l_j]) \oplus \bigoplus_{L_{j\infty} \in \mathcal{L}_{\infty}} L^2([0, \infty)),$$

the elements of which can be written as columns $\psi = (f_j : L_j \in \mathcal{L}, g_j : L_{j\infty} \in \mathcal{L}_{\infty})^T$. We consider the dynamics governed by a Hamiltonian which acts as $-d^2/dx^2$ on each link. In order to make it a self-adjoint operator, boundary conditions

$$(U_j - I)\Psi_j + i(U_j + I)\Psi'_j = 0 \tag{1}$$

with unitary matrices U_j have to be imposed upon the vertices \mathcal{X}_j , where Ψ_j and Ψ'_j are vectors of the functional values and of the (outward) derivatives at the particular vertex, respectively. In other words, the domain of the Hamiltonian consists of all functions in $W^{2,2}(\mathcal{L} \oplus \mathcal{L}_{\infty})$ which satisfy conditions (1). We will speak about the described structure as of a *quantum graph* and as long as there is no danger of misunderstanding we will use for simplicity the symbol Γ again.

While the model is simple, dealing with a complicated graph may be nevertheless cumbersome. To make it easier we will employ a trick mentioned to our knowledge for

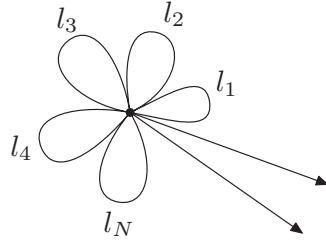


Figure 1. The model Γ_0 for a quantum graph Γ with N internal finite edges and M external links.

the first time in [Ku08] passing to a graph Γ_0 in which all edge ends meet in a single vertex as sketched in figure 1; the actual topology of Γ will be then encoded into the matrix which describes the coupling in the vertex.

To be more specific, suppose that Γ described above has an adjacency matrix C_{ij} and that matrices U_j describe the coupling between vectors of functional values Ψ_j and derivatives Ψ'_j at \mathcal{X}_j . This will correspond to the ‘flower-like’ graph with one vertex, the set of loops isomorphic to \mathcal{L} and the set of semi-infinite links \mathcal{L}_∞ which does not change; coupling at the only vertex of this graph is given by a ‘big’ unitary matrix U .

Denoting $N = \text{card } \mathcal{L}$ and $M = \text{card } \mathcal{L}_\infty$ we introduce the $(2N + M)$ -dimensional vector of functional values by $\Psi = (\Psi_1^T, \dots, \Psi_{\text{card } \mathcal{L}}^T)^T$ and similarly the vector of derivatives Ψ' at the vertex. The valency of this vertex is $M + \sum_{i,j} C_{ij} = 2N + M$. One can easily check that conditions (1) can be rewritten on Γ_0 using one $(2N + M) \times (2N + M)$ unitary block diagonal matrix U consisting of blocks U_j as

$$(U - I)\Psi + i(U + I)\Psi' = 0; \tag{2}$$

equation (2) obviously decouples into the set of equations (1) for Ψ_j and Ψ'_j .

Since neither the edge lengths and the corresponding Hilbert spaces nor the operator action on them is affected and the only change is a possible edge renumbering, the quantum graph Γ_0 is related to the original Γ by the natural unitary equivalence and the spectral properties we are interested in are not affected by the model modification.

2.2. Equivalence of the scattering and resolvent resonances

As another preliminary, we need a few facts about resonances on quantum graphs. In [EL06] we studied the situation where to each vertex of a compact graph at most one external semi-infinite link is attached; we have demonstrated that the resonances may be equivalently understood as poles of the analytically continued resolvent, $(H - \lambda \text{id})^{-1}$, or of the on-shell scattering matrix. Here we extend the result to all quantum graphs with a finite number of edges, both finite and semi-infinite: we will show that the resolvent and scattering resonances again coincide. The above-described ‘flower-like’ graph model allows us to give an elegant proof of this claim.

Let us begin with the resolvent resonances. As in [EL06] the idea is to employ an exterior complex scaling; this seminal idea can be traced back to the work of Combes and co-authors, cf [AC71], and its use in the graph setting is particularly simple. Looking for complex eigenvalues of the scaled operator we do not change the compact-graph part: using the Ansatz $f_j(x) = a_j \sin kx + b_j \cos kx$ on the internal edges we obtain

$$f_j(0) = b_j, \quad f_j(l_j) = a_j \sin kl_j + b_j \cos kl_j, \tag{3}$$

$$f'_j(0) = ka_j, \quad -f'_j(l_j) = -ka_j \cos kl_j + kb_j \sin kl_j; \tag{4}$$

hence, we have

$$\begin{pmatrix} f_j(0) \\ f_j(l_j) \end{pmatrix} = \begin{pmatrix} 0 & 1 \\ \sin kl_j & \cos kl_j \end{pmatrix} \begin{pmatrix} a_j \\ b_j \end{pmatrix}, \quad (5)$$

$$\begin{pmatrix} f'_j(0) \\ -f'_j(l_j) \end{pmatrix} = k \begin{pmatrix} 1 & 0 \\ -\cos kl_j & \sin kl_j \end{pmatrix} \begin{pmatrix} a_j \\ b_j \end{pmatrix}. \quad (6)$$

On the other hand, the functions on the semi-infinite edges are scaled by $g_{j\theta}(x) = e^{\theta/2}g_j(xe^\theta)$ with an imaginary θ rotating the essential spectrum of the transformed (non-self-adjoint) Hamiltonian into the lower complex half-plane so that the poles of the resolvent on the second sheet become ‘uncovered’ if the rotation angle is large enough. The argument is standard, both generally and in the graph setting [EL06], so we skip the details. In particular, the ‘exterior’ boundary values are given by

$$g_j(0) = e^{-\theta/2}g_{j\theta}, \quad g'_j(0) = ik e^{-\theta/2}g_{j\theta}. \quad (7)$$

Now we substitute equations (5), (6) and (7) into (2). We rearrange the terms in Ψ and Ψ' in such a way that the functional values corresponding to the two ends of each edge are neighboring, and the entries of the matrix U are rearranged accordingly. This yields

$$(U - I)C_1(k) \begin{pmatrix} a_1 \\ b_1 \\ a_2 \\ \vdots \\ b_N \\ e^{-\theta/2}g_{1\theta} \\ \vdots \\ e^{-\theta/2}g_{M\theta} \end{pmatrix} + ik(U + I)C_2(k) \begin{pmatrix} a_1 \\ b_1 \\ a_2 \\ \vdots \\ b_N \\ e^{-\theta/2}g_{1\theta} \\ \vdots \\ e^{-\theta/2}g_{M\theta} \end{pmatrix} = 0, \quad (8)$$

where the matrices C_1, C_2 are given by $C_1(k) = \text{diag}(C_1^{(1)}(k), C_1^{(2)}(k), \dots, C_1^{(N)}(k), I_{M \times M})$ and $C_2 = \text{diag}(C_2^{(1)}(k), C_2^{(2)}(k), \dots, C_2^{(N)}(k), iI_{M \times M})$, respectively, where

$$C_1^{(j)}(k) = \begin{pmatrix} 0 & 1 \\ \sin kl_j & \cos kl_j \end{pmatrix}, \quad C_2^{(j)}(k) = \begin{pmatrix} 1 & 0 \\ -\cos kl_j & \sin kl_j \end{pmatrix}$$

and $I_{M \times M}$ is an $M \times M$ unit matrix.

The solvability condition of the system (8) determines the eigenvalues of a scaled non-self-adjoint operator, and *mutatis mutandis* the poles of the analytically continued resolvent of the original graph Hamiltonian.

The other standard approach to resonances is to study poles of the on-shell scattering matrix, again in the lower complex half-plane. In our particular case we choose a combination of two planar waves, $g_j = c_j e^{-ikx} + d_j e^{ikx}$, as an Ansatz on the external edges; we ask about poles of the matrix $S = S(k)$ which maps the vector of amplitudes of the incoming waves $c = \{c_n\}$ into the vector of the amplitudes of the outgoing waves $d = \{d_n\}$ by $d = Sc$. The condition for the scattering resonances is then $\det S^{-1} = 0$ for appropriate complex values of k . The functional values and derivatives at the vertices are now given by

$$g_j(0) = c_j + d_j, \quad g'_j(0) = ik(d_j - c_j),$$

together with equations (3)–(4). After substituting into (2) one arrives at the condition

$$(U - I)C_1(k) \begin{pmatrix} a_1 \\ b_1 \\ a_2 \\ \vdots \\ b_N \\ c_1 + d_1 \\ \vdots \\ c_M + d_M \end{pmatrix} + ik(U + I)C_2(k) \begin{pmatrix} a_1 \\ b_1 \\ a_2 \\ \vdots \\ b_N \\ d_1 - c_1 \\ \vdots \\ d_M - c_M \end{pmatrix} = 0.$$

Since we are interested in zeros of $\det S^{-1}$, we regard the previous relation as an equation for variables a_j, b_j and d_j while c_j are just parameters; in other words,

$$[(U - I)C_1(k) + ik(U + I)C_2(k)] \begin{pmatrix} a_1 \\ b_1 \\ a_2 \\ \vdots \\ b_N \\ d_1 \\ \vdots \\ d_M \end{pmatrix} = [-(U - I)C_1(k) + ik(U + I)C_2(k)] \begin{pmatrix} 0 \\ 0 \\ \vdots \\ 0 \\ c_1 \\ \vdots \\ c_M \end{pmatrix}.$$

Eliminating the variables a_j, b_j one can derive from here a system of M equations expressing the map $S^{-1}d = c$. The condition under which the previous system is not solvable, what is equal to $\det S^{-1} = 0$, reads

$$\det [(U - I)C_1(k) + ik(U + I)C_2(k)] = 0 \tag{9}$$

being the same as the condition of solvability of the system (8); this means that the families of resonances determined in the two ways coincide.

2.3. Effective coupling on the finite graph

The study of resonances can be further simplified by reducing it to a problem on the compact subgraph only. The idea is to replace the coupling at the vertex where external semi-infinite edges are attached by an effective one obtained by eliminating the external variables. Substituting (7) into equation (2) we get

$$(U - I) \begin{pmatrix} f_1 \\ \vdots \\ f_{2N} \\ e^{-\theta/2}g_{1\theta} \\ \vdots \\ e^{-\theta/2}g_{M\theta} \end{pmatrix} + (U + I) \text{diag}(i, \dots, i, -k, \dots, -k) \begin{pmatrix} f'_1 \\ \vdots \\ f'_{2N} \\ e^{-\theta/2}g_{1\theta} \\ \vdots \\ e^{-\theta/2}g_{M\theta} \end{pmatrix} = 0. \tag{10}$$

We consider now U as a matrix consisting of four blocks, $U = \begin{pmatrix} U_1 & U_2 \\ U_3 & U_4 \end{pmatrix}$, where U_1 is the $2N \times 2N$ square matrix referring to the compact subgraph, U_4 is the $M \times M$ square matrix

related to the exterior part and U_2 and U_3 are rectangular matrices of the size $M \times 2N$ and $2N \times M$, respectively, connecting the two. Then the previous set of equations can be written as

$$V(f_1, \dots, f_{2N}, f'_1, \dots, f'_{2N}, e^{-\theta/2}g_{1\theta}, \dots, e^{-\theta/2}g_{M\theta})^T = 0,$$

where

$$V = \begin{pmatrix} U_1 - I & i(U_1 + I) & (1 - k)U_2 \\ U_3 & iU_3 & (1 - k)U_4 - (k + 1)I \end{pmatrix}.$$

If the matrix $[(1 - k)U_4 - (k + 1)I]$ is regular, one obtains from here

$$(e^{-\theta/2}g_{1\theta}, \dots, e^{-\theta/2}g_{M\theta})^T = -[(1 - k)U_4 - (k + 1)I]^{-1}U_3(f_1 + if'_1, \dots, f_{2N} + if'_{2N})^T$$

and substituting it further into (10) we find that the following expression

$$\begin{aligned} & \{U_1 - I - (1 - k)U_2[(1 - k)U_4 - (k + 1)I]^{-1}U_3\}(f_1, \dots, f_{2N})^T \\ & + i\{U_1 + I - (1 - k)U_2[(1 - k)U_4 - (k + 1)I]^{-1}U_3\}(f'_1, \dots, f'_{2N})^T = 0 \end{aligned}$$

must vanish. Consequently, elimination of the external part leads to an effective coupling on the compact part of the graph expressed by the condition

$$(\tilde{U}(k) - I)(f_1, \dots, f_{2N})^T + i(\tilde{U}(k) + I)(f'_1, \dots, f'_{2N})^T = 0,$$

where the corresponding coupling matrix

$$\tilde{U}(k) = U_1 - (1 - k)U_2[(1 - k)U_4 - (k + 1)I]^{-1}U_3 \quad (11)$$

is obviously energy dependent and, in general, may not be unitary.

3. Embedded eigenvalues for graphs with rationally related edges

As mentioned in the introduction, quantum graphs of the type we consider here have the positive half-line as the essential spectrum, and they may have eigenvalues with compactly supported eigenfunctions embedded in it.

3.1. A general result

We will focus on graphs which contain several internal edges of lengths equal to integer multiples of a fixed $l_0 > 0$. In the spirit of the previous section we restrict ourselves only to compact graphs remembering that the presence of an exterior part can be rephrased through an effective energy-dependent coupling replacing the original U by the matrix $\tilde{U}(k)$ defined above.

Following section 2.1 we model a given compact Γ by Γ_0 having only one vertex and N finite edges emanating from this vertex and ending at it. The coupling between the edges is described by a $2N \times 2N$ unitary matrix U and condition (2). Suppose that the lengths of the first n edges are integer multiples of a positive real number l_0 . Our aim is to find out for which matrices U the spectrum of the corresponding Hamiltonian $H = H_U$ contains the eigenvalues $k = 2m\pi/l_0$, $m \in \mathbb{N}$.

Since our graph is not directed, it is convenient to work in a setting invariant with respect to interchange of the edge ends. To this aim we choose the Ansatz

$$\Psi_j(x) = A_j \sin k(x - l_j/2) + B_j \cos k(x - l_j/2)$$

on the j th edge. Subsequently, one gets

$$\begin{pmatrix} \Psi_j(0) \\ \Psi_j(l_j) \end{pmatrix} = \begin{pmatrix} -\sin \frac{kl_j}{2} & \cos \frac{kl_j}{2} \\ \sin \frac{kl_j}{2} & \cos \frac{kl_j}{2} \end{pmatrix} \begin{pmatrix} A_j \\ B_j \end{pmatrix},$$

$$\begin{pmatrix} \Psi'_j(0) \\ -\Psi'_j(l_j) \end{pmatrix} = k \begin{pmatrix} \cos \frac{kl_j}{2} & \sin \frac{kl_j}{2} \\ -\cos \frac{kl_j}{2} & \sin \frac{kl_j}{2} \end{pmatrix} \begin{pmatrix} A_j \\ B_j \end{pmatrix}.$$

The eigenvalue condition, expressed in terms of solvability of the system (2), is given by

$$\det [UD_1(k) + D_2(k)] = 0, \tag{12}$$

where

$$D_1(k) = \begin{pmatrix} -\sin \frac{kl_1}{2} + ik \cos \frac{kl_1}{2} & \cos \frac{kl_1}{2} + ik \sin \frac{kl_1}{2} & \dots & 0 & 0 \\ \sin \frac{kl_1}{2} - ik \cos \frac{kl_1}{2} & \cos \frac{kl_1}{2} + ik \sin \frac{kl_1}{2} & \dots & 0 & 0 \\ \vdots & \vdots & \ddots & \vdots & \vdots \\ 0 & 0 & \dots & -\sin \frac{kl_N}{2} + ik \cos \frac{kl_N}{2} & \cos \frac{kl_N}{2} + ik \sin \frac{kl_N}{2} \\ 0 & 0 & \dots & \sin \frac{kl_N}{2} - ik \cos \frac{kl_N}{2} & \cos \frac{kl_N}{2} + ik \sin \frac{kl_N}{2} \end{pmatrix},$$

$$D_2(k) = \begin{pmatrix} \sin \frac{kl_1}{2} + ik \cos \frac{kl_1}{2} & -\cos \frac{kl_1}{2} + ik \sin \frac{kl_1}{2} & \dots & 0 & 0 \\ -\sin \frac{kl_1}{2} - ik \cos \frac{kl_1}{2} & -\cos \frac{kl_1}{2} + ik \sin \frac{kl_1}{2} & \dots & 0 & 0 \\ \vdots & \vdots & \ddots & \vdots & \vdots \\ 0 & 0 & \dots & \sin \frac{kl_N}{2} + ik \cos \frac{kl_N}{2} & -\cos \frac{kl_N}{2} + ik \sin \frac{kl_N}{2} \\ 0 & 0 & \dots & -\sin \frac{kl_N}{2} - ik \cos \frac{kl_N}{2} & -\cos \frac{kl_N}{2} + ik \sin \frac{kl_N}{2} \end{pmatrix}.$$

For a future purpose, let us rewrite the spectral condition (12) in the form $\det (C(k) + S(k)) = 0$, where the matrix $C(k)$ contains terms with $\cos \frac{kl_j}{2}$ and $S(k)$ contains those with $\sin \frac{kl_j}{2}$. Hence, all the entries in the first $2n$ columns of $S(k)$ vanish for $k = 2m\pi/l_0, m \in \mathbb{N}$, while the others can be nontrivial. Similarly, all the entries in the first $2n$ columns of $C(k)$ are for $k = (2m + 1)\pi/l_0, m \in \mathbb{N}$, equal to zero. The entries of the ‘cosine’ matrix are

$$C_{i,2j-1}(k) = (u_{i,2j-1} - u_{i,2j})ik \cos \frac{kl_j}{2} + (\delta_{i,2j-1} - \delta_{i,2j})ik \cos \frac{kl_j}{2},$$

$$C_{i,2j}(k) = (u_{i,2j-1} + u_{i,2j}) \cos \frac{kl_j}{2} - (\delta_{i,2j-1} + \delta_{i,2j}) \cos \frac{kl_j}{2}.$$

Similarly, the entries of $S(k)$ are

$$S_{i,2j-1}(k) = (-u_{i,2j-1} + u_{i,2j}) \sin \frac{kl_j}{2} + (\delta_{i,2j-1} - \delta_{i,2j}) \sin \frac{kl_j}{2},$$

$$S_{i,2j}(k) = (u_{i,2j-1} + u_{i,2j})ik \sin \frac{kl_j}{2} + (\delta_{i,2j-1} + \delta_{i,2j})ik \sin \frac{kl_j}{2}.$$

First of all, let us consider the situation when $\sin kl_0/2 = 0$.

Theorem 3.1. *Let a graph Γ_0 consist of a single vertex and N finite edges emanating from this vertex and ending at it, and suppose that the coupling between the edges is described by*

a $2N \times 2N$ unitary matrix U and condition (2). Let the lengths of the first n edges be integer multiples of a positive real number l_0 . If the rectangular $2N \times 2n$ matrix

$$M_{\text{even}} = \begin{pmatrix} u_{11} & u_{12} - 1 & u_{13} & u_{14} & \cdots & u_{1,2n-1} & u_{1,2n} \\ u_{21} - 1 & u_{22} & u_{23} & u_{24} & \cdots & u_{2,2n-1} & u_{2,2n} \\ u_{31} & u_{32} & u_{33} & u_{34} - 1 & \cdots & u_{3,2n-1} & u_{3,2n} \\ u_{41} & u_{42} & u_{43} - 1 & u_{44} & \cdots & u_{4,2n-1} & u_{4,2n} \\ \vdots & \vdots & \vdots & \vdots & \ddots & \vdots & \vdots \\ u_{2N-1,1} & u_{2N-1,2} & u_{2N-1,3} & u_{2N-1,4} & \cdots & u_{2N-1,2n-1} & u_{2N-1,2n} \\ u_{2N,1} & u_{2N,2} & u_{2N,3} & u_{2N,4} & \cdots & u_{2N,2n-1} & u_{2N,2n} \end{pmatrix} \quad (13)$$

has rank smaller than $2n$, then the spectrum of the corresponding Hamiltonian $H = H_U$ contains eigenvalues of the form $\epsilon = 4m^2\pi^2/l_0^2$ with $m \in \mathbb{N}$ and the multiplicity of these eigenvalues is at least the difference between $2n$ and the rank of M_{even} .

Proof. Condition (12) is clearly satisfied if the rectangular matrix containing only the first $2n$ columns has rank smaller than $2n$, because then some of the columns of matrix $C(k) + S(k)$ are linearly dependent. Since all the entries of the first $2n$ columns of $S(k)$ contain the term $\sin kl_j/2$, which disappears for $kl_0 = 2m\pi$, one can consider the matrix $C(k)$ only. Dividing some of the columns of $C(k)$ by appropriate nonzero terms, which is possible since $\cos kl_j/2 \neq 0$ for $\sin kl_0/2 = 0$, and subtracting them from each other does not change the rank of the matrix. This argument shows that the rank of the matrix M_{even} must be smaller than $2n$ in order to yield a solution of condition (12) and that the multiplicity is given by the difference. \square

It is important to note that the unitarity of U played no role in the argument, and consequently, one can obtain in this way embedded eigenvalues $\epsilon = 4m^2\pi^2/l_0^2$ for a graph containing external links; however, the matrix $M_{\text{even}}(k)$ defined in analogy with (13) must have rank smaller than $2n$ for all values of k .

Mathematically speaking the described case does not involve only cases where the original graph Γ contains a loop with rational rate of the lengths of the edges. Choosing appropriate U one can find such eigenvalues also for graphs where the edges of Γ with lengths equal to integer multiples of l_0 are not adjacent. This corresponds, however, to couplings allowing the particle to ‘hop’ between different vertices which is not so interesting from the point of view of the underlying physical model.

A similar claim can be made also for kl_0 equal to odd multiples of π .

Theorem 3.2. *If under the same assumptions as above, the rectangular $2N \times 2n$ matrix*

$$M_{\text{odd}} = \begin{pmatrix} u_{11} & u_{12} + 1 & u_{13} & u_{14} & \cdots & u_{1,2n-1} & u_{1,2n} \\ u_{21} + 1 & u_{22} & u_{23} & u_{24} & \cdots & u_{2,2n-1} & u_{2,2n} \\ u_{31} & u_{32} & u_{33} & u_{34} + 1 & \cdots & u_{3,2n-1} & u_{3,2n} \\ u_{41} & u_{42} & u_{43} + 1 & u_{44} & \cdots & u_{4,2n-1} & u_{4,2n} \\ \vdots & \vdots & \vdots & \vdots & \ddots & \vdots & \vdots \\ u_{2N-1,1} & u_{2N-1,2} & u_{2N-1,3} & u_{2N-1,4} & \cdots & u_{2N-1,2n-1} & u_{2N-1,2n} \\ u_{2N,1} & u_{2N,2} & u_{2N,3} & u_{2N,4} & \cdots & u_{2N,2n-1} & u_{2N,2n} \end{pmatrix}, \quad (14)$$

has rank smaller than $2n$, then the spectrum of the corresponding Hamiltonian $H = H_U$ contains eigenvalues of the form $\epsilon = (2m + 1)^2\pi^2/l_0^2$ with $m \in \mathbb{N}$ and the multiplicity of these eigenvalues is at least the difference between $2n$ and rank of M_{odd} .

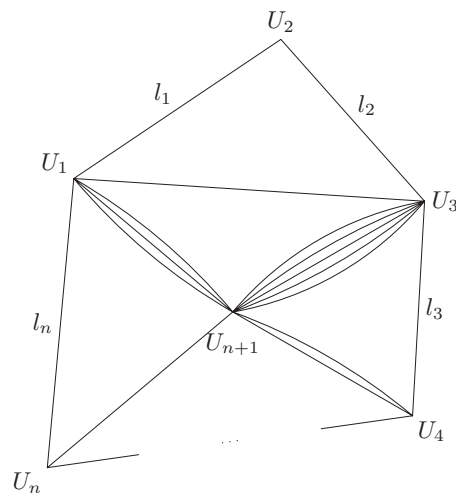


Figure 2. A loop of the edges with rational rate of their lengths.

We skip the proof which is similar to the previous one, the change being that the roles of the matrices $S(k)$ and $C(k)$ are interchanged. We also note that similarly as above the results extend to graphs with semi-infinite external edges.

3.2. A loop with δ or δ'_s couplings

As mentioned above, a prime example of embedded eigenvalues in the considered class of quantum graphs concerns the situation when Γ contains a subgraph in the form of a loop of n edges with the lengths equal to integer multiples of l_0 . We denote by $U_j, j = 1, \dots, n$, the unitary matrices describing the coupling at the vertices of such a loop and by U_{n+1} the unitary matrix which describes the coupling at all the other vertices of the graph—cf figure 2. The unitary matrix which describes the coupling on the whole graph, in the sense explained in section 2.1, is

$$U = \begin{pmatrix} U_1 & 0 & \dots & 0 \\ 0 & U_2 & \dots & 0 \\ \vdots & \vdots & \ddots & \vdots \\ 0 & 0 & \dots & U_{n+1} \end{pmatrix}.$$

Let us further restrict our attention to the case when the coupling in the loop vertices is *invariant with respect to the permutation of edges*, i.e. suppose that matrices U_1, \dots, U_n can be written as $U_j = a_j J + b_j I$, where I is a unit matrix, J is a matrix with all entries equal to 1 and a_j and b_j are complex numbers satisfying $|b_j| = 1$ and $|b_j + a_j \deg \mathcal{X}_j| = 1$ to make the operator self-adjoint—cf [ET07].

Recall that in order to use theorems 3.1 and 3.2 one has to rearrange the columns and rows of the unitary matrix U accordingly. The first $2n$ entries in Ψ and Ψ' correspond to the edges with rational rates of their lengths. Therefore, appropriate permutations of columns and rows of U must be performed: the first two columns should correspond to the first edge of the

loop (from the vertex 1 to 2), the second two columns to the second edge, etc. The rearranged coupling matrix is thus $\begin{pmatrix} U_r & 0 \\ 0 & U_{n+1} \end{pmatrix}$ with

$$U_r = \begin{pmatrix} a_1 + b_1 & 0 & 0 & \dots & 0 & 0 & a_1 & a_1 & \dots & a_1 & 0 & \dots & 0 & 0 & \dots & 0 \\ 0 & a_2 + b_2 & a_2 & \dots & 0 & 0 & 0 & 0 & \dots & 0 & a_2 & \dots & a_2 & 0 & \dots & 0 \\ 0 & a_2 & a_2 + b_2 & \dots & 0 & 0 & 0 & 0 & \dots & 0 & a_2 & \dots & a_2 & 0 & \dots & 0 \\ \vdots & \vdots & \vdots & \ddots & \vdots & \vdots & \vdots & \vdots & \ddots & \vdots & \vdots & \ddots & \vdots & \vdots & \ddots & \vdots \\ 0 & 0 & 0 & \dots & a_n + b_n & a_n & 0 & 0 & \dots & 0 & 0 & \dots & 0 & a_n & \dots & a_n \\ 0 & 0 & 0 & \dots & a_n & a_n + b_n & 0 & 0 & \dots & 0 & 0 & \dots & 0 & a_n & \dots & a_n \\ a_1 & 0 & 0 & \dots & 0 & 0 & a_1 + b_1 & a_1 & \dots & a_1 & 0 & \dots & 0 & 0 & \dots & 0 \\ a_1 & 0 & 0 & \dots & 0 & 0 & a_1 & a_1 + b_1 & \dots & a_1 & 0 & \dots & 0 & 0 & \dots & 0 \\ \vdots & \vdots & \vdots & \ddots & \vdots & \vdots & \vdots & \vdots & \ddots & \vdots & \vdots & \ddots & \vdots & \vdots & \ddots & \vdots \\ a_1 & 0 & 0 & \dots & 0 & 0 & a_1 & a_1 & \dots & a_1 + b_1 & 0 & \dots & 0 & 0 & \dots & 0 \\ 0 & a_2 & a_2 & \dots & 0 & 0 & 0 & 0 & \dots & 0 & a_2 + b_2 & \dots & a_2 & 0 & \dots & 0 \\ \vdots & \vdots & \vdots & \ddots & \vdots & \vdots & \vdots & \vdots & \ddots & \vdots & \vdots & \ddots & \vdots & \vdots & \ddots & \vdots \\ 0 & a_2 & a_2 & \dots & 0 & 0 & 0 & 0 & \dots & 0 & a_2 & \dots & a_2 + b_2 & 0 & \dots & 0 \\ \vdots & \vdots & \vdots & \ddots & \vdots & \vdots & \vdots & \vdots & \ddots & \vdots & \vdots & \ddots & \vdots & \vdots & \ddots & \vdots \\ 0 & 0 & 0 & \dots & a_n & a_n & 0 & 0 & \dots & 0 & 0 & \dots & 0 & a_n + b_n & \dots & a_n \\ \vdots & \vdots & \vdots & \ddots & \vdots & \vdots & \vdots & \vdots & \ddots & \vdots & \vdots & \ddots & \vdots & \vdots & \ddots & \vdots \\ 0 & 0 & 0 & \dots & a_n & a_n & 0 & 0 & \dots & 0 & 0 & \dots & 0 & a_n & \dots & a_n + b_n \end{pmatrix}.$$

The corresponding matrix M_{even} is constructed in the way described in the previous section. It consists of a nontrivial $2n \times 2n$ part (U_r with added -1's) and $\text{deg } \mathcal{X}_1 - 2$ copies of the row $(a_1, 0, \dots, 0, a_1)$, $\text{deg } \mathcal{X}_2 - 2$ copies of the row $(0, a_2, a_2, 0, \dots, 0)$, etc, and, finally, its last $\text{deg } \mathcal{X}_{n+1}$ rows have all the entries equal to zero; hence, the total number of its rows is $2N$ as required.

If all the a_j 's are nonzero, the condition $\text{rank } M_{\text{even}} < 2n$ simplifies to

$$\text{rank} \begin{pmatrix} b_1 & -1 & 0 & 0 & \dots & 0 & 0 & 0 \\ -1 & b_2 & 0 & 0 & \dots & 0 & 0 & 0 \\ 0 & 0 & b_2 & -1 & \dots & 0 & 0 & 0 \\ 0 & 0 & -1 & b_3 & \dots & 0 & 0 & 0 \\ \vdots & \vdots & \vdots & \vdots & \ddots & \vdots & \vdots & \vdots \\ 0 & 0 & 0 & 0 & \dots & b_n & 0 & 0 \\ 0 & 0 & 0 & 0 & \dots & 0 & b_n & -1 \\ 0 & 0 & 0 & 0 & \dots & 0 & -1 & b_1 \\ 1 & 0 & 0 & 0 & \dots & 0 & 0 & 1 \\ 0 & 1 & 1 & 0 & \dots & 0 & 0 & 0 \\ \vdots & \vdots & \vdots & \vdots & \ddots & \vdots & \vdots & \vdots \\ 0 & 0 & 0 & 0 & \dots & 1 & 1 & 0 \end{pmatrix} < 2n.$$

It is easy to see that the assumptions of theorem 3.1 giving rise to eigenvalues corresponding to $kl_0 = 2\pi m$ are satisfied in the case $b_j = -1, \forall j \in \{1, \dots, N\}$, which corresponds

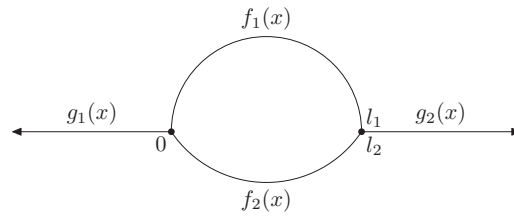


Figure 3. A loop with two leads.

to δ -couplings. The counterpart case, $b_j = 1$, corresponding to δ'_s couplings leads to the requirement

$$\text{rank} \begin{pmatrix} 1 & 1 & 0 & 0 & 0 & \dots & 0 & 0 & 0 \\ 0 & 1 & -1 & 0 & 0 & \dots & 0 & 0 & 0 \\ 0 & 0 & 1 & 1 & 0 & \dots & 0 & 0 & 0 \\ 0 & 0 & 0 & 1 & -1 & \dots & 0 & 0 & 0 \\ \vdots & \vdots & \vdots & \vdots & \vdots & \ddots & \vdots & \vdots & \vdots \\ 0 & 0 & 0 & 0 & 0 & \dots & 1 & -1 & 0 \\ 0 & 0 & 0 & 0 & 0 & \dots & 0 & 1 & 1 \\ -1 & 0 & 0 & 0 & 0 & \dots & 0 & 0 & 1 \end{pmatrix} < 2n,$$

which is satisfied if and only if the number of the edges in the loop is even.

In a similar way, one can prove that eigenvalues corresponding to $kl_0 = (2m + 1)\pi$ are present in the spectrum of a graph with δ'_s -couplings on the loop, while for δ -couplings this is true provided the loop consists of an even number of the edges.

If there are several half-lines attached to the loop and all the b_j 's are equal to -1 or $+1$, respectively, we obtain the same results as before. One can easily check that for $U = aJ + bI$ all entries of the energy-dependent part

$$(1 - k)U_2[(1 - k)U_4 - (k + 1)I]^{-1}U_3$$

of the effective coupling matrix $\tilde{U}(k)$ given by (11) are equal; hence, the matrix \tilde{U} can be written using multiples of the matrices J and I and the coefficient b is not energy dependent, i.e. $\tilde{U} = \tilde{a}(k)J + \tilde{b}I$. Since the coefficients a_j can be eliminated from the final condition, we obtain the same results as in the energy-independent case.

Note that the case $b_j = -1$ also includes an array of edges with rationally related lengths and Dirichlet condition at both the array endpoints. In this case one of the matrices describing the coupling is $U_j = \text{diag}(-1, -1)$. Similarly, $b_j = 1$ includes the case of an edge array with Neumann conditions at both the endpoints, the corresponding matrix being $U_j = \text{diag}(1, 1)$.

4. Examples

As stated in the introduction, our main goal is to analyze resonances which arise from the above-discussed embedded eigenvalues if the rational relation between the graph edge lengths is perturbed. Let us look now at this effect in two simple examples.

4.1. A loop with two leads

Consider first the graph sketched in figure 3 consisting of two internal edges of lengths l_1, l_2 and one half-line connected to each endpoint. The Hamiltonian acts as $-d^2/dx^2$ on each link.

The corresponding Hilbert space is $L^2(\mathbb{R}^+) \oplus L^2(\mathbb{R}^+) \oplus L^2([0, l_1]) \oplus L^2([0, l_2])$; states of the system are described by columns $\psi = (g_1, g_2, f_1, f_2)^T$. For a greater generality, let us consider the following coupling conditions [ES89] which include the δ -coupling but also allow the attachment of the semi-infinite links to the loop to be tuned, and possibly to be turned off:

$$\begin{aligned} f_1(0) &= f_2(0), & f_1(l_1) &= f_2(l_2), \\ f_1(0) &= \alpha_1^{-1}(f_1'(0) + f_2'(0)) + \gamma_1 g_1'(0), \\ f_1(l_1) &= -\alpha_2^{-1}(f_1'(l_1) + f_2'(l_2)) + \gamma_2 g_2'(0), \\ g_1(0) &= \bar{\gamma}_1(f_1'(0) + f_2'(0)) + \bar{\alpha}_1^{-1} g_1'(0), \\ g_2(0) &= -\bar{\gamma}_2(f_1'(l_1) + f_2'(l_2)) + \bar{\alpha}_2^{-1} g_2'(0). \end{aligned}$$

Following the construction described in section 2 and parametrizing the internal edges by $l_1 = l(1-\lambda)$, $l_2 = l(1+\lambda)$, $\lambda \in [0, 1]$ —which effectively means shifting one of the connections points around the loop as λ is changing—one arrives at the final condition for resonances in the form

$$\begin{aligned} \sin kl(1-\lambda) \sin kl(1+\lambda) - 4k^2 \beta_1^{-1}(k) \beta_2^{-1}(k) \sin^2 kl \\ + k[\beta_1^{-1}(k) + \beta_2^{-1}(k)] \sin 2kl = 0, \end{aligned} \quad (15)$$

where $\beta_i^{-1}(k) := \alpha_i^{-1} + \frac{ik|\gamma_i|^2}{1-ik\bar{\alpha}_i^{-1}}$.

We are interested in how the solutions to the above condition change with respect to change of the length parameter $\lambda \rightarrow \lambda' = \lambda + \varepsilon$. It is easy to check that any solution k depends on ε continuously, and therefore for small ε we can thus construct a perturbation expansion. Let k_0 be a solution of (15) for λ and k be a solution for λ' ; the difference $\kappa = k - k_0$ can be obtained using the Taylor expansion

$$\begin{aligned} \kappa l [\sin(2k_0 l) - \lambda \sin(2k_0 l \lambda)] - 4\kappa l k_0^2 \beta_1^{-1}(k_0) \beta_2^{-1}(k_0) \sin 2k_0 l \\ - 4\kappa [2k_0 \beta_1^{-1}(k_0) \beta_2^{-1}(k_0) + k_0^2 (\beta_1^{-1}(k_0) \tilde{\beta}_2(k_0) + \tilde{\beta}_1(k_0) \beta_2^{-1}(k_0))] \sin^2 k_0 l \\ + \kappa (\beta_1^{-1}(k_0) + \beta_2^{-1}(k_0) + \tilde{\beta}_1(k_0) k_0 + \tilde{\beta}_2(k_0) k_0) \sin 2k_0 l + 2\kappa l k_0 (\beta_1^{-1}(k_0) \\ + \beta_2^{-1}(k_0)) \cos 2k_0 l - \kappa l [\varepsilon \cos k_0 l \varepsilon \sin k_0 l (2\lambda + \varepsilon) \\ + (2\lambda + \varepsilon) \cos k_0 l (2\lambda + \varepsilon) \sin k_0 l \varepsilon] + \mathcal{O}(\kappa^2) = \sin k_0 l (2\lambda + \varepsilon) \sin k_0 l \varepsilon, \end{aligned} \quad (16)$$

where $\tilde{\beta}_j(k_0) = i|\gamma_j|^2 / (1 - ik_0 \bar{\alpha}_j^{-1})^2$. This equation can be used to determine κ in the leading order. Denoting the coefficient of κ by $f(k_0)$ and the rhs of the above equation by $g(\lambda, \varepsilon)$ we find that the error in such an evaluation is

$$\delta = \frac{\mathcal{O}(\kappa^2)}{f(k_0)} = \frac{1}{f(k_0)} \mathcal{O}\left(\frac{g^2(\lambda, \varepsilon)}{f^2(k_0, \varepsilon)}\right).$$

Since the rhs of (16) is $\mathcal{O}(\varepsilon)$ as $\varepsilon \rightarrow 0$, the error we make by neglecting the term $\mathcal{O}(\kappa^2)$ is $\mathcal{O}(\varepsilon^2)$. In fact, in the vicinity of the embedded eigenvalues, i.e. for $2\lambda k_0 l$ close to $= 2n\pi$ the error is even smaller, namely $\mathcal{O}(\varepsilon^4)$ as we will see below.

In fact, we can get more from equation (16) than just the perturbative expansion. We are interested in the global behavior, i.e. trajectories of the resonance poles in the lower complex half-plane as λ changes. To obtain them one should solve equation (15) numerically, since an analytic solution is available in exceptional cases only. One can, however, also solve numerically the approximate equation (16) starting from $\lambda = \frac{m}{n}$ where the corresponding embedded eigenvalues given by $kl = n\pi$ are present, and taking ε perturbations of the successive solutions. This method is simple and we have employed it in the examples below, with a sufficiently small step, $\varepsilon = 5 \times 10^{-5}$. To check the consistency, we have compared the results of the second example with a direct numerical solution of equation (15) found with the

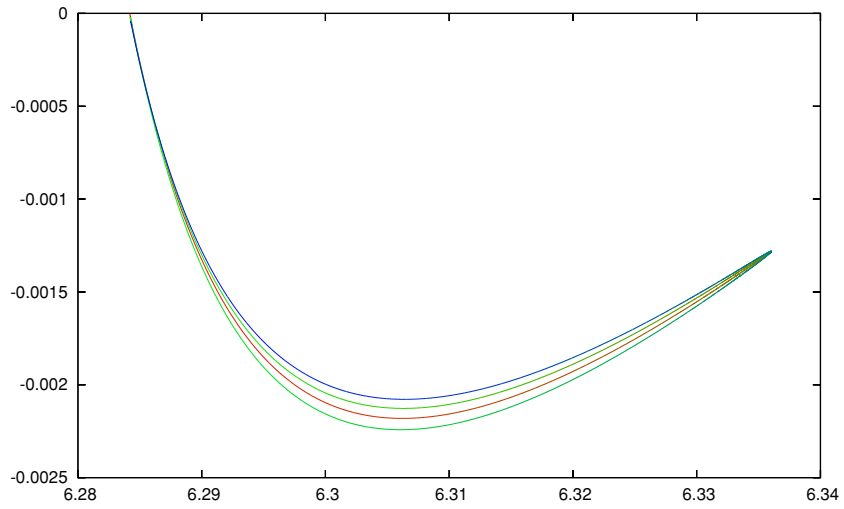


Figure 4. The trajectory of the resonance pole in the lower complex half-plane starting from $k_0 = 2\pi$ corresponding to $\lambda = 0$ for $l = 1$ and the coefficient values $\alpha_1^{-1} = 1, \tilde{\alpha}_1^{-1} = -2, |\gamma_1|^2 = 1, \alpha_2^{-1} = 0, \tilde{\alpha}_2^{-1} = 1, |\gamma_2|^2 = 1, n = 2$. The color coding shows the dependence on λ changing from red ($\lambda = 0$) to blue ($\lambda = 1$).

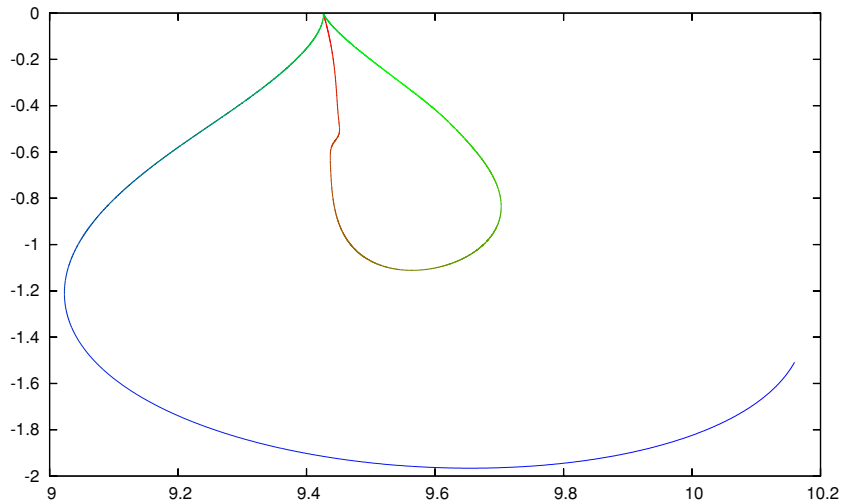


Figure 5. The trajectory of the resonance pole starting at $k_0 = 3\pi$ corresponding to $\lambda = 0$ for the coefficient values $\alpha_1^{-1} = 1, \alpha_2^{-1} = 1, \tilde{\alpha}_1^{-1} = 1, \tilde{\alpha}_2^{-1} = 1, |\gamma_1|^2 = |\gamma_2|^2 = 1, n = 3$. The color coding is the same as in the previous picture.

step 0.05 in the parameter λ , and found that they give closely similar results, the relative error being of order of 10^{-3} .

Examples of poles trajectories obtained in the described way from equation (16) are shown in figures 4–6. Equation (15) has the real solution $kl = n\pi, n \in \mathbb{N}$, for $\lambda = m/n, m \in \mathbb{N}$; the corresponding eigenfunction is $\psi = (0, 0, \sin n\pi x/l, -\sin n\pi x/l)^T$. In figure 4 corresponding to $n = 2$ the pole returns to the real axis when $\lambda = 1/2$ and $\lambda = 1$. On

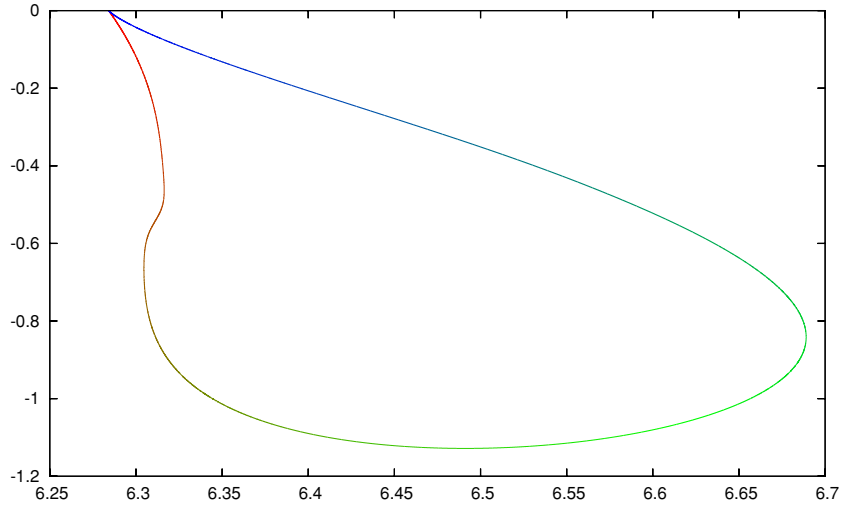


Figure 6. The trajectory of the resonance pole starting at $k_0 = 2\pi$ corresponding to $\lambda = 0$ for the coefficient values $\alpha_1^{-1} = 1, \alpha_2^{-1} = 1, \tilde{\alpha}_1^{-1} = 1, \tilde{\alpha}_2^{-1} = 1, |\gamma_1|^2 = 1, |\gamma_2|^2 = 1, n = 2$. The color coding is the same as in figures 4 and 5.

the other hand, figure 5 with $n = 3$ shows the situation when the pole returns to the real axis only for $\lambda = 2/3$, while for $\lambda = 1/3$ and $\lambda = 1$ the appropriate solution is a resonance. Similarly, the pole shown in figure 6 where $n = 2$ returns to the real axis only if $\lambda = 1$. To show how fast the poles are moving, the change of the parameter λ from 0 to 1 is marked by changing the color from red ($\lambda = 0$) to blue ($\lambda = 1$).

Let us now investigate the asymptotic behavior of the resonances in the vicinity of the embedded eigenvalue, in particular, the angle φ between the pole trajectory emerging from $k_0 = n\pi/l$ with $\lambda_0 = m/n, m \in \{0, 1, \dots, n\}$, and the real axis. For small κ the difference $\varepsilon = \lambda - \lambda_0$ is also small. We use a rewritten form of condition (15):

$$f(k, \lambda) = \cos 2kl\lambda - \cos 2kl - 8k^2\beta_1^{-1}(k)\beta_2^{-1}(k)\sin^2 kl + 2k(\beta_1^{-1}(k) + \beta_2^{-1}(k))\sin 2kl = 0. \tag{17}$$

The function $f(k, \lambda)$ is, with the exception of points $k = -i\tilde{\alpha}_j$, continuous and its first partial derivative with respect to λ at λ_0 is equal to zero; hence,

$$0 = f(k, \lambda) \approx f(k_0, \lambda_0) + \frac{\partial^2 f}{\partial \lambda^2} \Big|_{k_0, \lambda_0} \varepsilon^2 + \frac{\partial f}{\partial k} \Big|_{k_0, \lambda_0} \kappa,$$

$$\frac{\partial f}{\partial k} \Big|_{(k_0, \lambda_0)} = 4n\pi [\beta_1^{-1}(k_0) + \beta_2^{-1}(k_0)],$$

$$\frac{\partial^2 f}{\partial \lambda^2} \Big|_{(k_0, \lambda_0)} = -4(kl)^2 \cos 2kl\lambda = -4(\pi n)^2.$$

For small κ we obtain using (16)

$$\kappa \approx \varepsilon^2 \frac{\pi n}{\beta_1^{-1}(k_0) + \beta_2^{-1}(k_0)},$$

$$\tan \varphi = \frac{\text{Im } \kappa}{\text{Re } \kappa} = \frac{\frac{k_0|\gamma_1|^2}{1+k_0^2\tilde{\alpha}_1^{-2}} + \frac{k_0|\gamma_2|^2}{1+k_0^2\tilde{\alpha}_2^{-2}}}{\alpha_1^{-1} + \alpha_2^{-1} - \frac{k_0^2|\gamma_1|^2\tilde{\alpha}_1^{-1}}{1+k_0^2\tilde{\alpha}_1^{-2}} - \frac{k_0^2|\gamma_2|^2\tilde{\alpha}_2^{-1}}{1+k_0^2\tilde{\alpha}_2^{-2}}}, \quad k_0 = \frac{n\pi}{l}. \tag{18}$$

For $|\gamma_1| = |\gamma_2| = 0$ the poles are real and $\varphi = 0$; this is the case when the loop and the leads are decoupled and the eigenvalues remain embedded. On the other hand, if $\alpha_1^{-1} = \tilde{\alpha}_1^{-1} = \alpha_2^{-1} = \tilde{\alpha}_2^{-1} = 0$, then the real part of κ is zero and the pole trajectory goes from k_0 perpendicular to the horizontal line, i.e. $\varphi = \pi/2$.

Furthermore, let us investigate the behavior of the pole trajectories' height in the spectrum, i.e. for large values of n . Suppose that $k = k_0 + \kappa$, $k_0 = n\pi/l$, $|\kappa| \ll \pi/l$; then

$$\begin{aligned} \cos 2kl\lambda - \cos 2kl &= \cos 2k_0l\lambda \cos 2\kappa l\lambda - \sin 2k_0l\lambda \sin 2\kappa l\lambda - \cos 2\kappa l \\ &= (\cos 2n\pi\lambda - 1) - \sin(2\pi n\lambda)2\kappa l\lambda + \mathcal{O}(\kappa^2). \end{aligned}$$

Condition (17) for small κ becomes

$$(\cos 2n\pi\lambda - 1) - \sin(2\pi n\lambda)2\kappa l\lambda + 2\frac{n\pi}{l}[\beta_1^{-1}(k_0) + \beta_2^{-1}(k_0)]2\kappa l + \mathcal{O}(\kappa^2) = 0.$$

Using the expressions of coefficients $\beta_j(k)$, we obtain

$$\begin{aligned} \beta_j^{-1}(k_0) &= \alpha_j^{-1} - \frac{|\gamma_j|^2}{\tilde{\alpha}_j^{-1}} + i\frac{l|\gamma_j|^2}{n\pi\tilde{\alpha}_j^{-2}} + \mathcal{O}(n^{-2}) \quad \text{for } \tilde{\alpha}_j^{-1} \neq 0, \\ \beta_j^{-1}(k_0) &= i\frac{n\pi}{l}|\gamma_j|^2 + \mathcal{O}(1) \quad \text{for } \tilde{\alpha}_j^{-1} = 0. \end{aligned}$$

The quantities appearing above,

$$|\cos(2n\pi\lambda) - 1| \leq 2 \quad \text{and} \quad |\sin(2\pi n\lambda)| \leq 1,$$

are bounded; thus for $\tilde{\alpha}_1^{-1} \neq 0$ and $\tilde{\alpha}_2^{-1} \neq 0$, we have

$$|\text{Im}\kappa| \leq \frac{l}{2(\pi n)^2} \frac{|\gamma_1|^2/\tilde{\alpha}_1^{-2} + |\gamma_2|^2/\tilde{\alpha}_2^{-2}}{(\alpha_1^{-1} + \alpha_2^{-1} - |\gamma_1|^2/\tilde{\alpha}_1^{-1} - |\gamma_2|^2/\tilde{\alpha}_2^{-1})^2} + \mathcal{O}(n^{-3}),$$

while for $\tilde{\alpha}_1^{-1} = 0$ and $\tilde{\alpha}_2^{-1} = 0$ the inequality reads

$$|\text{Im}\kappa| \leq \frac{l}{2(\pi n)^2} \frac{1}{|\gamma_1|^2 + |\gamma_2|^2} + \mathcal{O}(n^{-3}),$$

and for $\tilde{\alpha}_1^{-1} = 0$, $\tilde{\alpha}_2^{-1} \neq 0$ we have

$$|\text{Im}\kappa| \leq \frac{l}{2(\pi n)^2} \frac{1}{|\gamma_1|^2} + \mathcal{O}(n^{-3}).$$

Let us summarize the discussion of this example. The poles of the resolvent are given by condition (15), or equivalently, by (17). If $\lambda = m/n$, $m \in \mathbb{N}$, real eigenvalues corresponding to $kl = n\pi$, $n \in \mathbb{N}$, occur. They may correspond to a particular pole of the resolvent returning to the real axis for $\lambda = m/n$, $m \in \mathbb{N}$, as in figure 4. However, for other coupling conditions, the pole may return only for certain λ , see figures 5 and 6, while for other rational λ its place may be taken by the pole which has been a resonance for $\lambda = 0$. The angle between the resonance trajectory and the real axis does not depend on λ and is given by (18). If the pole trajectory is near the original eigenvalue, then the distance from the real axis is of order of $\mathcal{O}(n^{-2})$ for large n .

4.2. A cross-shaped graph

Let us now consider another simple graph, this time consisting of two leads and two internal edges attached to the leads at one point, cf figure 7; the lengths of the internal edges are $l_1 = l(1 - \lambda)$ and $l_2 = l(1 + \lambda)$.

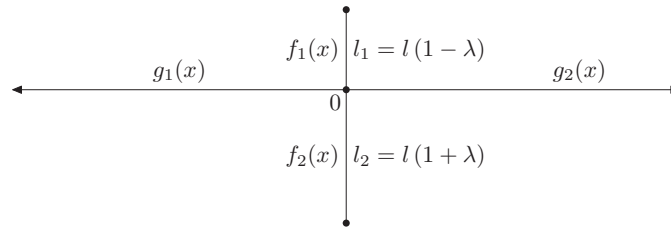


Figure 7. A cross-shaped resonator.

The Hamiltonian acts again as $-d^2/dx^2$ on the corresponding Hilbert space $L^2(\mathbb{R}^+) \oplus L^2(\mathbb{R}^+) \oplus L^2([0, l_1]) \oplus L^2([0, l_2])$, and the states are described by columns $\psi = (g_1, g_2, f_1, f_2)^T$. This time we restrict ourselves to the δ coupling as the boundary condition at the vertex and we consider Dirichlet conditions at the loose ends, i.e.

$$\begin{aligned} f_1(0) &= f_2(0) = g_1(0) = g_2(0), \\ f_1(l_1) &= f_2(l_2) = 0, \\ \alpha f_1(0) &= f_1'(0) + f_2'(0) + g_1'(0) + g_2'(0). \end{aligned}$$

Using the same technique as above we arrive at two equivalent forms of the condition for resonances: $k \sin 2kl + (\alpha - 2ik) \sin kl(1 - \lambda) \sin kl(1 + \lambda) = 0$ or

$$2k \sin 2kl + (\alpha - 2ik)(\cos 2kl\lambda - \cos 2kl) = 0. \tag{19}$$

Let us ask when the solution is real. Leaving out the trivial case $k = 0$ we get from the last equation two conditions referring to the vanishing of the real and imaginary parts of the lhs:

$$\begin{aligned} \sin 2kl = 0 &\Rightarrow kl = \frac{n\pi}{2}, \quad n \in \mathbb{Z}, \\ 0 = \cos 2kl\lambda - \cos 2kl &= \cos n\pi\lambda - \cos n\pi = 2 \sin \frac{n\pi}{2}(1 - \lambda) \sin \frac{n\pi}{2}(1 + \lambda) \\ &\Rightarrow n\lambda = (n - 2m), \quad m \in \mathbb{Z}. \end{aligned}$$

Hence, $\lambda = 1 - 2m/n$, $m \in \mathbb{N}_0$, $m \leq n/2$.

If the difference $\kappa = k - k_0$ is small, we obtain from (19)

$$\begin{aligned} \kappa \approx &-2(\alpha - 2ik_0) \sin k_0 l \varepsilon \sin k_0 l (2\lambda + \varepsilon) \{2i[\cos 2k_0 l (\lambda + \varepsilon) - \cos 2k_0 l] \\ &+ (\alpha - 2ik_0) 2l[(\lambda + \varepsilon) \sin 2k_0 l (\lambda + \varepsilon) - \sin 2k_0 l] - 2 \sin 2k_0 l - 4k_0 l \cos 2k_0 l\}^{-1}. \end{aligned} \tag{20}$$

Similarly as in the previous example, the error here is $\mathcal{O}(\kappa^2)$, i.e. $\mathcal{O}(\varepsilon^2)$, and for $2\lambda k_0 l$ close to $= 2n\pi$ it is even smaller, namely $\mathcal{O}(\varepsilon^4)$. In the latter case, the above expression for $k_0 = n\pi/l$, $\lambda = m/n$ and small ε yield

$$\kappa \approx -\frac{2(\alpha - 2ik_0)(k_0 l \varepsilon)^2}{-4k_0 l} = \frac{n\pi \varepsilon^2}{2} \left(\alpha - 2i \frac{n\pi}{l} \right).$$

The slope of the pole trajectory at its start from k_0 is equal to

$$\tan \varphi = -\frac{\text{Im } \kappa}{\text{Re } \kappa} = \frac{2n\pi}{\alpha l} \Rightarrow \varphi = \arctan \frac{2n\pi}{\alpha l}. \tag{21}$$

As we have said, the embedded eigenvalues occur in accordance with (19) at $kl = n\pi/2$, $n \in \mathbb{Z}$, for $\lambda = 1 - 2m/n$, $m \in \mathbb{N}_0$, $m \leq n/2$. The geometric perturbation gives rise to pole trajectories which can be found from (19), or from (20) with a sufficiently small step. Examples worked out using the second method are shown in figures 8–10. We see that a resolvent pole may return to the same point, or it may become another eigenvalue or a resonance. Another interesting type of behavior, an avoided resonance crossing, can be seen in figure 10.

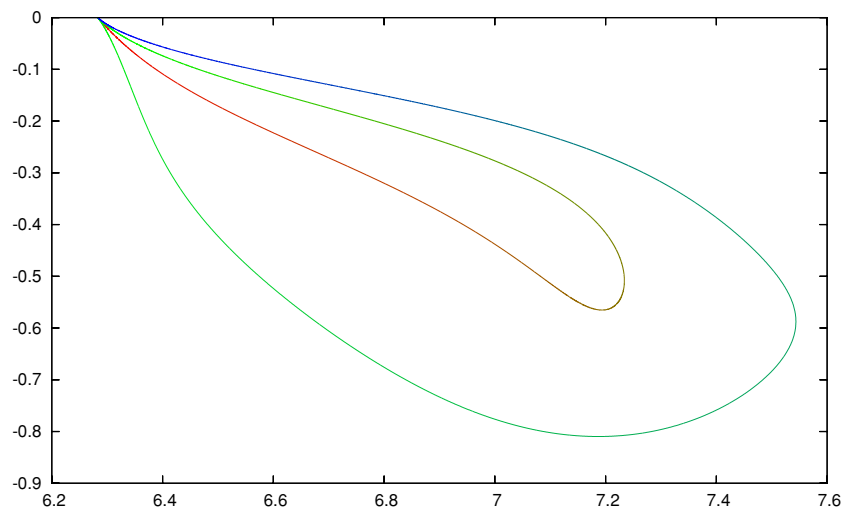


Figure 8. The trajectory of the resonance pole starting at $k_0 = 2\pi$ for the coefficient values $\alpha = 10, n = 2$. The color coding is the same as in the previous figures.

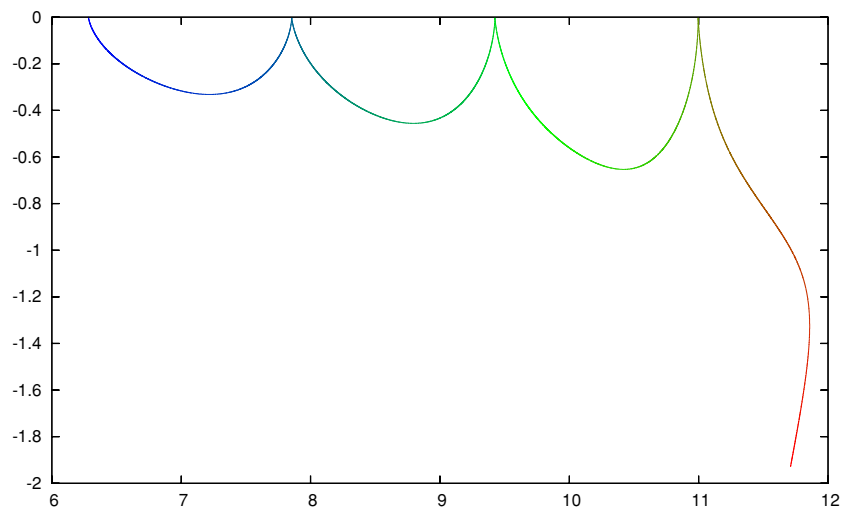


Figure 9. The trajectory of the resonance pole for the coefficient values $\alpha = 1, n = 2$. The color coding is the same as above.

5. The general case

After analyzing the above two examples, let us look what could be said about the geometric perturbation problem in the general case.

5.1. Multiplicity of the eigenvalues

Suppose that k_0 is an eigenvalue of multiplicity d embedded in a continuous spectrum of H . First we will assume that $k_0 l_0 = 2\pi m$. Our aim is now to determine whether k_0 is still

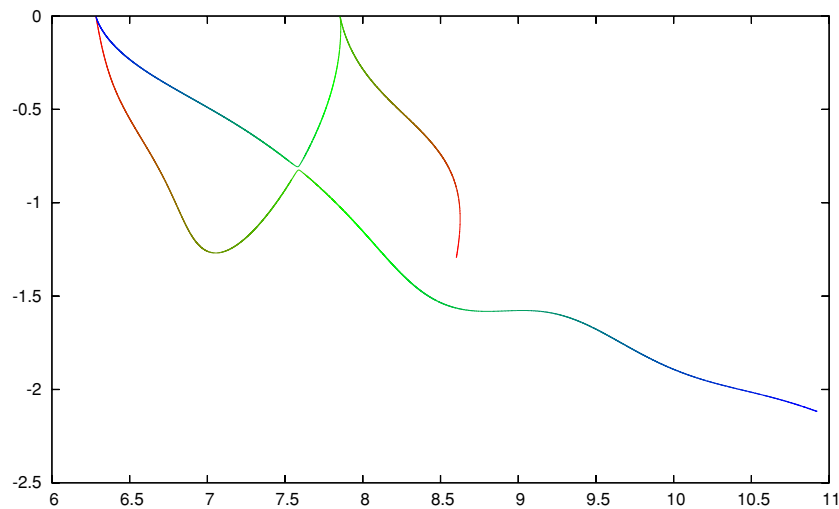


Figure 10. The trajectories of two resonance poles for the coefficient values $\alpha = 2.596$, $n = 2$. We can see an avoided resonance crossing—the former eigenvalue ‘traveling from the left to the right’ interchanges with the former resonance ‘traveling the other way’ and ending up as an embedded eigenvalue. The color coding is the same as in previous figures.

eigenvalue (and what is its multiplicity) if the lengths of the graph edges are perturbed. We will write the lengths as $l'_j = l_0(n_j + \varepsilon_j)$ assuming that $n_j \in \mathbb{N}$ for $j \in \{1, \dots, n\}$, while n_j is not an integer for $j \in \{n + 1, \dots, N\}$.

From the construction described in the proof of theorem 3.1 we find that condition (13) is not affected by small length variations of the ‘noninteger’ edges, $j \in \{n + 1, \dots, N\}$. Hence, the number of rationality related eigenvalues of the perturbed graph referring to the first n edges does not depend on perturbations of the other edge lengths. The spectral condition (12) can be written as $\det J(k) = 0$ if we put $J(k) := C(k) + S(k)$. Using the expansion

$$\begin{aligned} ik \cos \frac{kl_0(n_j + \varepsilon_j)}{2} \mp \sin \frac{kl_0(n_j + \varepsilon_j)}{2} \\ = \cos \frac{k_0 l_0 n_j}{2} \left(ik_0 \cos \frac{k_0 l_0 \varepsilon_j}{2} \mp \sin \frac{k_0 l_0 \varepsilon_j}{2} \right) + \mathcal{O}(k - k_0), \end{aligned}$$

and an analogous one for $\cos \frac{kl_0(n_j + \varepsilon_j)}{2} + ik \sin \frac{kl_0(n_j + \varepsilon_j)}{2}$ one finds that the entries of $J(k)$ can be rewritten as

$$\begin{aligned} J_{i,2j-1}(k) &= (u_{i,2j-1} - u_{i,2j}) \cos \frac{k_0 l_0 n_j}{2} \left(ik_0 \cos \frac{k_0 l_0 \varepsilon_j}{2} - \sin \frac{k_0 l_0 \varepsilon_j}{2} \right) \\ &\quad + (\delta_{i,2j-1} - \delta_{i,2j}) \cos \frac{k_0 l_0 n_j}{2} \left(ik_0 \cos \frac{k_0 l_0 \varepsilon_j}{2} + \sin \frac{k_0 l_0 \varepsilon_j}{2} \right) + \mathcal{O}(k - k_0) \\ J_{i,2j}(k) &= (u_{i,2j-1} + u_{i,2j}) \cos \frac{k_0 l_0 n_j}{2} \left(\cos \frac{k_0 l_0 \varepsilon_j}{2} + ik_0 \sin \frac{k_0 l_0 \varepsilon_j}{2} \right) \\ &\quad + (\delta_{i,2j-1} + \delta_{i,2j}) \cos \frac{k_0 l_0 n_j}{2} \left(-\cos \frac{k_0 l_0 \varepsilon_j}{2} + ik_0 \sin \frac{k_0 l_0 \varepsilon_j}{2} \right) + \mathcal{O}(k - k_0). \end{aligned}$$

For small enough ε_j ’s and a real nonzero noninteger k_0 the terms $\cos \frac{k_0 l_0 n_j}{2}$, $ik_0 \cos \frac{k_0 l_0 \varepsilon_j}{2} - \sin \frac{k_0 l_0 \varepsilon_j}{2}$ and $\cos \frac{k_0 l_0 \varepsilon_j}{2} + ik_0 \sin \frac{k_0 l_0 \varepsilon_j}{2}$ are nonzero. After dividing the columns of $J(k)$ by these

terms and using the arguments from the proof of theorem 3.1 one arrives at the following conclusion.

Theorem 5.1. *In the setting of theorem 3.1 suppose that the rank of M_{even} is smaller than $2n$. Let us vary the edge lengths, $l'_j = l_0(n_j + \varepsilon_j)$, with sufficiently small ε_j 's; then the multiplicity of the eigenvalues $\epsilon = k_0^2 = 4m^2\pi^2/l_0^2$ due to rationality of the first n edges is given by the difference between $2n$ and the rank of the matrix:*

$$M_{\text{even}}^{\{\varepsilon_j\}} = \begin{pmatrix} u_{11} + \tilde{\varepsilon}_1^a & u_{12} - 1 + \tilde{\varepsilon}_1^b & u_{13} & u_{14} & \cdots & u_{1,2n-1} & u_{1,2n} \\ u_{21} - 1 + \tilde{\varepsilon}_1^b & u_{22} + \tilde{\varepsilon}_1^a & u_{23} & u_{24} & \cdots & u_{2,2n-1} & u_{2,2n} \\ u_{31} & u_{32} & u_{33} + \tilde{\varepsilon}_2^a & u_{34} - 1 + \tilde{\varepsilon}_2^b & \cdots & u_{3,2n-1} & u_{3,2n} \\ u_{41} & u_{42} & u_{43} - 1 + \tilde{\varepsilon}_2^b & u_{44} + \tilde{\varepsilon}_2^a & \cdots & u_{4,2n-1} & u_{4,2n} \\ \vdots & \vdots & \vdots & \vdots & \ddots & \vdots & \vdots \\ u_{2N-1,1} & u_{2N-1,2} & u_{2N-1,3} & u_{2N-1,4} & \cdots & u_{2N-1,2n-1} & u_{2N-1,2n} \\ u_{2N,1} & u_{2N,2} & u_{2N,3} & u_{2N,4} & \cdots & u_{2N,2n-1} & u_{2N,2n} \end{pmatrix},$$

where

$$\tilde{\varepsilon}_j^a(k) := \frac{(1 - k_0^2) \sin k_0 l_0 \varepsilon_j}{2ik_0 \cos k_0 l_0 \varepsilon_j - (1 + k_0^2) \sin k_0 l_0 \varepsilon_j},$$

$$\tilde{\varepsilon}_j^b(k) := \frac{2ik_0(-1 + \cos k_0 l_0 \varepsilon_j) - (1 + k_0^2) \sin k_0 l_0 \varepsilon_j}{2ik_0 \cos k_0 l_0 \varepsilon_j - (1 + k_0^2) \sin k_0 l_0 \varepsilon_j}.$$

In a similar way one can treat the case when $k_0 l_0$ is equal to odd multiples of π . Then we employ the expansion

$$ik \cos \frac{kl_0(n_j + \varepsilon_j)}{2} \mp \sin \frac{kl_0(n_j + \varepsilon_j)}{2}$$

$$= \sin \frac{k_0 l_0 n_j}{2} \left(-ik_0 \sin \frac{k_0 l_0 \varepsilon_j}{2} \mp \cos \frac{k_0 l_0 \varepsilon_j}{2} \right) + \mathcal{O}(k - k_0)$$

and an analogous expression for $\cos \frac{kl_0(n_j + \varepsilon_j)}{2} + ik \sin \frac{kl_0(n_j + \varepsilon_j)}{2}$; with the help of them we arrive at the following conclusion.

Theorem 5.2. *In the setting of theorem 3.2 suppose that the rank of M_{odd} is smaller than $2n$. Passing to $l'_j = l_0(n_j + \varepsilon_j)$ with small enough ε_j 's, the multiplicity of the eigenvalues $\epsilon = k_0^2 = (2m + 1)^2\pi^2/l_0^2$ due to rationality of the first n edges is given by the difference between $2n$ and rank of a matrix:*

$$M_{\text{odd}}^{\{\varepsilon_j\}} = \begin{pmatrix} u_{11} + \tilde{\varepsilon}_1^a & u_{12} + 1 - \tilde{\varepsilon}_1^b & u_{13} & u_{14} & \cdots & u_{1,2n-1} & u_{1,2n} \\ u_{21} + 1 - \tilde{\varepsilon}_1^b & u_{22} + \tilde{\varepsilon}_1^a & u_{23} & u_{24} & \cdots & u_{2,2n-1} & u_{2,2n} \\ u_{31} & u_{32} & u_{33} + \tilde{\varepsilon}_2^a & u_{34} + 1 - \tilde{\varepsilon}_2^b & \cdots & u_{3,2n-1} & u_{3,2n} \\ u_{41} & u_{42} & u_{43} + 1 - \tilde{\varepsilon}_2^b & u_{44} + \tilde{\varepsilon}_2^a & \cdots & u_{4,2n-1} & u_{4,2n} \\ \vdots & \vdots & \vdots & \vdots & \ddots & \vdots & \vdots \\ u_{2N-1,1} & u_{2N-1,2} & u_{2N-1,3} & u_{2N-1,4} & \cdots & u_{2N-1,2n-1} & u_{2N-1,2n} \\ u_{2N,1} & u_{2N,2} & u_{2N,3} & u_{2N,4} & \cdots & u_{2N,2n-1} & u_{2N,2n} \end{pmatrix}$$

with $\tilde{\varepsilon}_j^a$ and $\tilde{\varepsilon}_j^b$ being defined in the previous theorem.

5.2. Total number of poles of the resolvent after perturbation

In general an embedded eigenvalue can split under the geometric perturbations considered here, a part of it being preserved with a lower multiplicity while the rest is turned into resonance(s). Above we have shown what the reduced multiplicity of the embedded eigenvalue is; now we complement this result by showing that the total number of poles produced in this way, multiplicity taken into account, remains locally preserved. Before stating the result, let us first demonstrate two useful lemmata.

Lemma 5.1. *Let $(k, \vec{\varepsilon}) \mapsto g(k, \vec{\varepsilon}) : \mathbb{C} \times \mathbb{R}^m \rightarrow \mathbb{C}$ be a function uniformly continuous in $\vec{\varepsilon}$ for all $\vec{\varepsilon} \in \mathcal{U}_{\varepsilon_0}(0)$ and $k \in \mathcal{U}_R(k_0)$, $\varepsilon_0 > 0$, $R > 0$, and holomorphic in k in $\mathcal{U}_R(k_0)$ for all $\vec{\varepsilon} \in \mathcal{U}_{\varepsilon_0}(0)$. Furthermore, let $\lim_{\vec{\varepsilon} \rightarrow 0} g(k, \vec{\varepsilon}) = (k - k_0)^d$. Then there exist such $\delta > 0$ and $\varepsilon'_0 > 0$ that for all $\vec{\varepsilon} \in \mathcal{U}_{\varepsilon'_0}(0)$ the sum of the multiplicities of zeros of $g(k, \vec{\varepsilon})$ in $\mathcal{U}_\delta(k_0)$ is d .*

Proof. Since g is holomorphic, we have the Taylor expansion

$$g(k, \vec{\varepsilon}) = \sum_{p=0}^{\infty} a_p(\varepsilon)(k - k_0)^p = P(k, \vec{\varepsilon}) + (k - k_0)^{d+1}h(k, \vec{\varepsilon}) = P(k, \vec{\varepsilon})[1 + (k - k_0)\tilde{h}(k, \vec{\varepsilon})],$$

where $P(k, \vec{\varepsilon})$ is a polynomial of order d in the variable k ; furthermore, $\lim_{\vec{\varepsilon} \rightarrow 0} h(k, \vec{\varepsilon}) = 0$ and $\lim_{\vec{\varepsilon} \rightarrow 0} \tilde{h}(k, \vec{\varepsilon}) = \lim_{\vec{\varepsilon} \rightarrow 0} (k - k_0)^d h(k, \vec{\varepsilon}) / P(k, \vec{\varepsilon}) = 0$. Due to the fundamental theorem of algebra $P(k, \vec{\varepsilon})$ has d zeros, not necessarily different, whose distance from k_0 depends continuously on $\vec{\varepsilon}$. On the other hand, we have $\forall \delta \exists \varepsilon'_0 : \forall \vec{\varepsilon} \in \mathcal{U}_{\varepsilon'_0}(0), \forall k \in \mathcal{U}_R(k_0) : |\tilde{h}(k, \vec{\varepsilon})| < \delta$ in view of the above limit relations; choosing then $\delta < 1/R$ we can conclude that zeros of the term $[1 + (k - k_0)\tilde{h}(k, \vec{\varepsilon})]$ lie outside the ball $\mathcal{U}_R(k_0)$. \square

The following lemma slightly generalizes the result to a larger class of $g(k, \vec{\varepsilon})$.

Lemma 5.2. *Let $(k, \vec{\varepsilon}) \mapsto F(k, \vec{\varepsilon}) : \mathbb{C} \times \mathbb{R}^m \rightarrow \mathbb{C}$ be a function uniformly continuous in $\vec{\varepsilon}$ for all $\vec{\varepsilon} \in \mathcal{U}_{\varepsilon_0}(0)$ and $k \in \mathcal{U}_R(k_0)$, $\varepsilon_0 > 0$, $R > 0$, and holomorphic in k in $\mathcal{U}_R(k_0)$ for all $\vec{\varepsilon} \in \mathcal{U}_{\varepsilon_0}(0)$. Suppose that $F(k, 0)$ has in $\mathcal{U}_R(k_0)$ a single zero of multiplicity d at the point k_0 ; then there exist such $\delta > 0$ and $\varepsilon'_0 > 0$ that for all $\vec{\varepsilon} \in \mathcal{U}_{\varepsilon'_0}(0)$ the sum of the multiplicities of zeros of $F(k, \vec{\varepsilon})$ in $\mathcal{U}_\delta(k_0)$ is equal to d .*

Proof. In view of the holomorphy of F and the fact that F has a zero of order d in k_0 one has $F(k, \vec{\varepsilon}) = (k - k_0)^d f(k, \vec{\varepsilon})$, where $\lim_{\vec{\varepsilon} \rightarrow 0} f(k, \vec{\varepsilon}) \neq 0$. Because f is continuous in $\vec{\varepsilon}$ we have $f(k, \vec{\varepsilon}) \neq 0$ for all $\vec{\varepsilon} \in \mathcal{U}_{\varepsilon'_0}(0)$, $k \in \mathcal{U}_R(k_0)$. Hence, f does not contribute to zeros of F in $\mathcal{U}_R(k_0)$ and lemma 5.1 can be used. \square

This conclusion allows us to demonstrate the indicated result. Our aim is to determine the number of resolvent poles, multiplicity counting, of the quantum graph with perturbed edge lengths in the neighborhood of an original pole of multiplicity d . In particular, we want to find out whether the number of solutions of condition (9)—into which we substitute from (11)—changes in the neighborhood of k_0 . In the notation of the previous lemma, the function F is given by the lhs of (9) and the vector $\vec{\varepsilon}$ describes the change of the edge lengths.

Theorem 5.3. *Let Γ be a quantum graph with N finite edges of the lengths l_i , M infinite edges and the coupling described by the matrix $U = \begin{pmatrix} U_1 & U_2 \\ U_3 & U_4 \end{pmatrix}$, where U_4 corresponds to the coupling between the infinite edges. Let k_0 satisfy $\det[(1 - k_0)U_4 - (1 + k_0)I] \neq 0$ and let k_0 be a pole of the resolvent $(H - \lambda \text{id})^{-1}$ of a multiplicity d . Let Γ_ε be a geometrically perturbed quantum graph with the edges of lengths $l_i(1 + \varepsilon)$ and the same coupling as Γ . Then there*

exists an $\varepsilon_0 > 0$ such that for all $\vec{\varepsilon} \in \mathcal{U}_{\varepsilon_0}(0)$ the sum of multiplicities of the resolvent poles in a sufficiently small neighborhood of k_0 is d .

Proof. One can rewrite condition (12) for poles of the resolvent into the form $F(k, \vec{\varepsilon}) = 0$, where $\vec{\varepsilon}$ is the vector of differences of the lengths of the internal edges. Using the form of the matrices $D_1(k)$ and $D_2(k)$ and equation (11) one can easily check that if $\det[(1 - k_0)U_4 - (1 + k_0)I] \neq 0$, then there exists a neighborhood $U_R(k_0)$ where $F(k_0, \vec{\varepsilon})$ is holomorphic in k and uniformly continuous in $\vec{\varepsilon}$; hence, lemma 5.2 can be applied. \square

Note that the condition $\det[(1 - k_0)U_4 - (1 + k_0)I] \neq 0$ is automatically satisfied for $k_0 \in \mathbb{R}^+$ because of the inequality $|(k_0 + 1)/(k_0 - 1)| > 1$ and the fact that the eigenvalues of U_4 do not exceed one in modulus.

Acknowledgments

The research was supported by the Czech Ministry of Education, Youth and Sports, within project LC06002. We thank the referee for suggestions which helped to improve the text.

References

- [AC71] Aguilar J and Combes J-M 1971 A class of analytic perturbations for one-body Schrödinger operators *Commun. Math. Phys.* **22** 269–79
- [EL06] Exner P and Lipovský J 2007 Equivalence of resolvent and scattering resonances on quantum graphs *Adventures in Mathematical Physics* vol 447 (*Proceedings, Cergy-Pontoise 2006*) (Providence, RI: American Mathematical Society) pp 73–81
- [ES89] Exner P and Šeba P 1989 Free quantum motion on a branching graph *Rep. Math. Phys.* **28** 7–26
- [ET07] Exner P and Turek O 2007 Approximations of singular vertex couplings in quantum graphs *Rev. Math. Phys.* **19** 571–606
- [Ku04,05] Kuchment P 2004 Quantum graphs: I. Some basic structures, II. Some spectral properties of quantum and combinatorial graphs *Waves Random Media* **14** S107–28
Kuchment P 2005 *J. Phys. A: Math. Gen.* **38** 269–79
- [Ku08] Kuchment P 2008 Quantum graphs: an introduction and a brief survey *Analysis on Graphs and Its Applications (Proc. Symp. Pure. Math.)* (Providence, RI: American Mathematical Society) pp 291–314